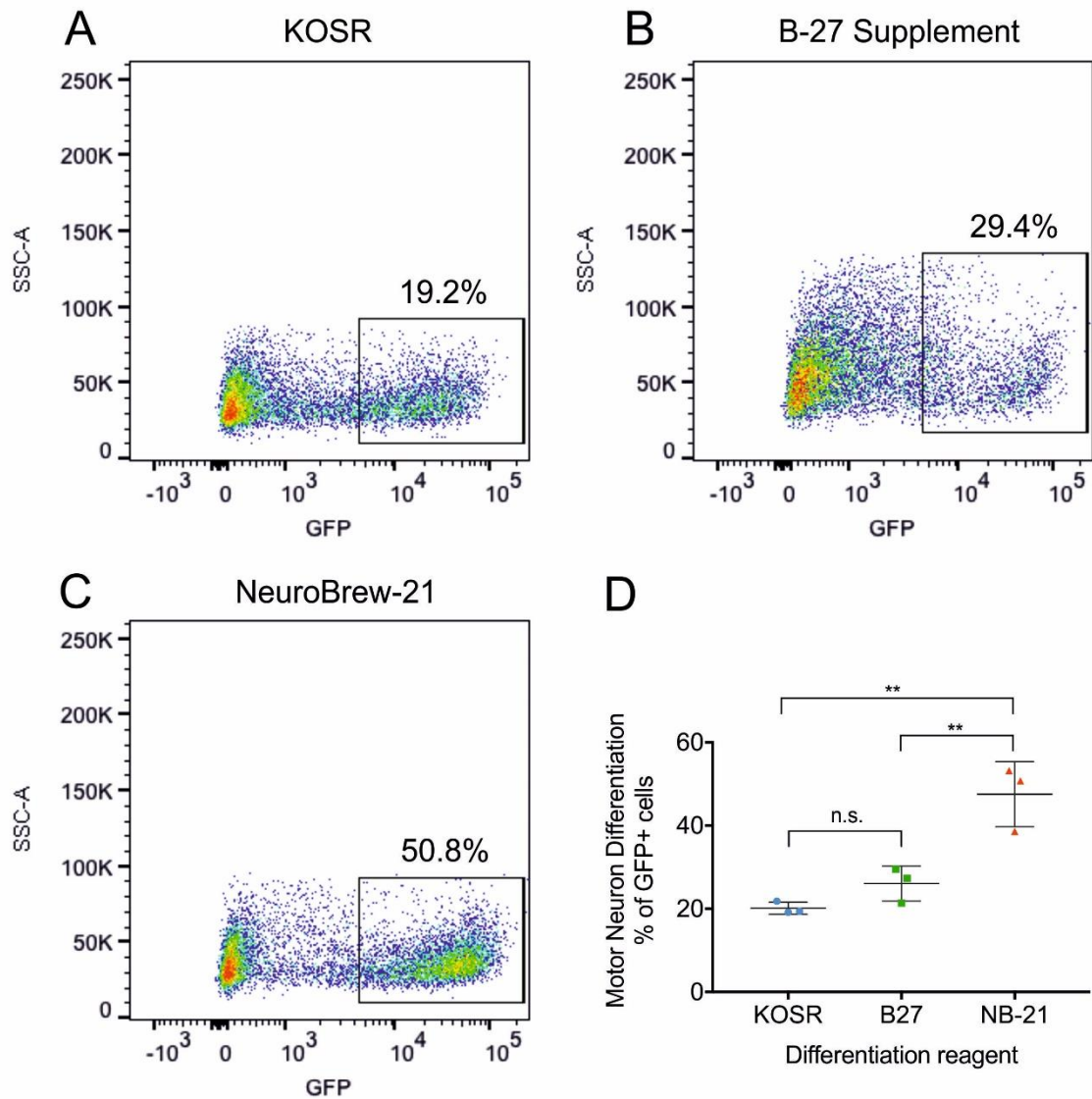
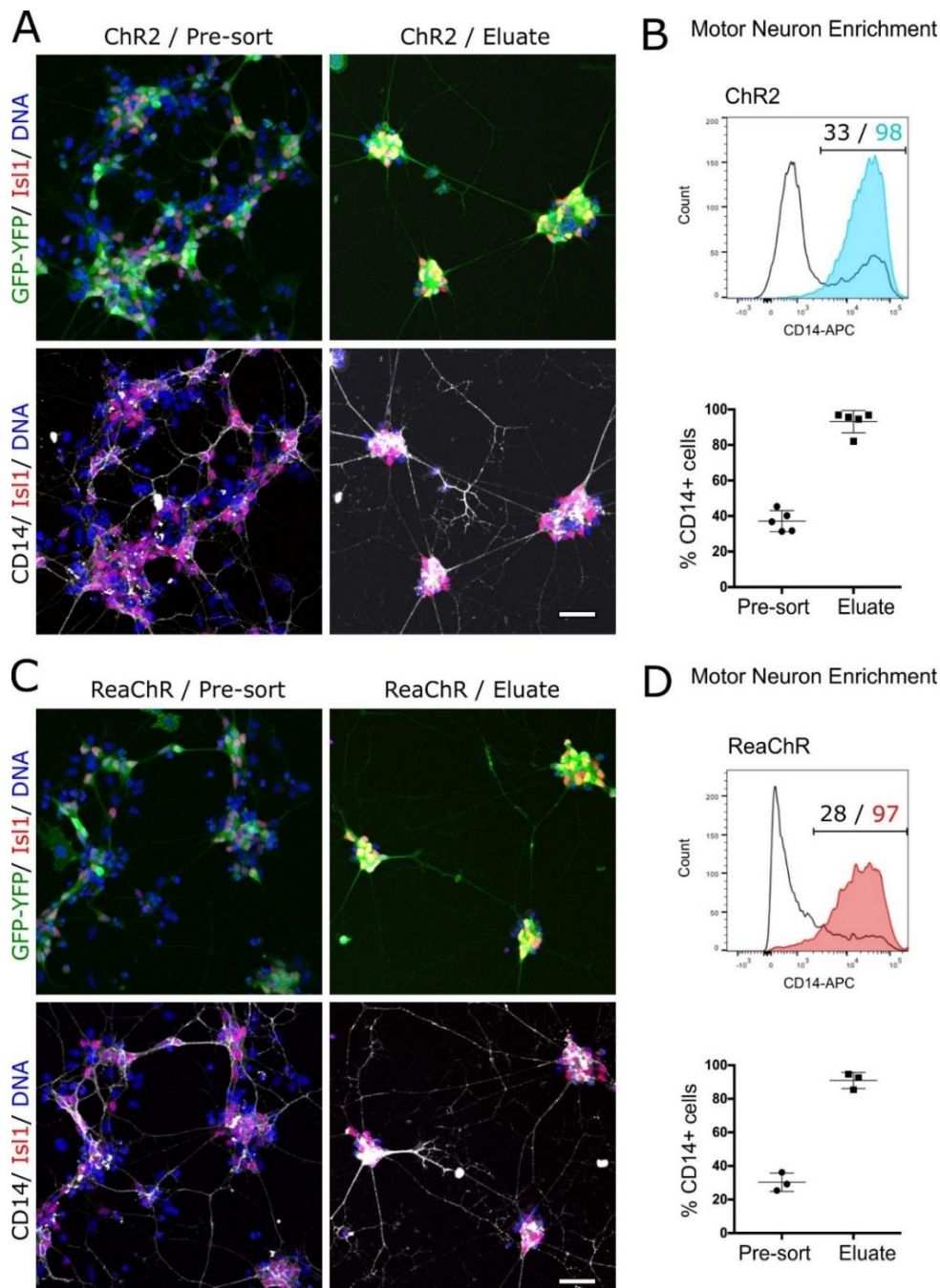


# Supporting Information



**Figure S1.** Impact of media composition on MN yield after ESC differentiation. FACS-analysis of *Hb9::CD14-IRES-GFP* ESCs differentiated into MN using (A) Knock-out serum replacement (KOSR), (B) N2 combined with B27 supplement or (C) N2 combined with MACS NeuroBrew-21 supplement. (D) Medium containing MACS NeuroBrew-21 (NB-21) generated a higher percentage of MNs than media containing B27 or KOSR (n=3 independent experiments). Two-way ANOVA with Tukey's multiple comparisons test, \*\*p<0.005, n.s. not significant. Lines indicate mean and SD.



**Figure S2.** Isolation of ChR2- and ReaChR-MNs from ESCs. (A) ChR2-MNs before and after enrichment by anti-CD14 MACS, scale bar 50 $\mu$ m. (B) Representative flow cytometry histograms of MACS enrichment show the percentage of sorted MNs in differentiation cultures prior (black) and after (blue) MACS. The graph shows the quantification of MN enrichment in n=5 independent experiments. (C) ReaChR-MNs before and after enrichment by MACS, scale bar 50 $\mu$ m. (D) Representative flow cytometry histograms of anti-CD14 MACS enrichment show the percentage of ReaChR-MN in differentiation cultures prior (black) and after (red) MACS. The graph shows the quantification of MN enrichment in n=3 independent experiments. Lines indicate mean and SD.

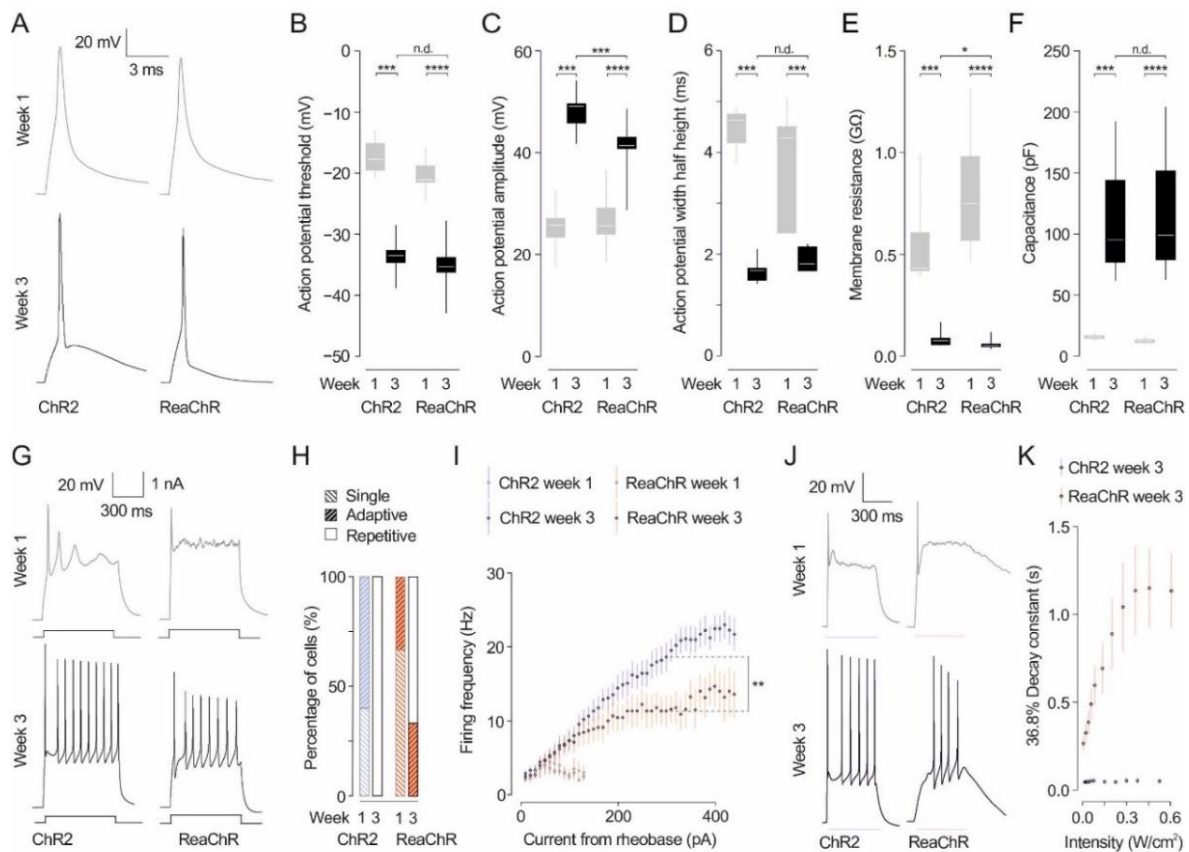


**Figure S3. Electrophysiological characterisation of ChR2- and ReaChR-MNs.** (A) Representative current-clamp recordings from ESC-derived MNs at 1 week (grey) or 3 weeks (black) post-differentiation. 1 ms of 1 nA current injections were used to elicit single action potentials. (B-F) Features of single action potentials described by box-and-whisker plots that indicate the median (white line), the 25th-75th percentiles (box edge), and the 10th-90th percentiles (whiskers); statistical analyses were performed using a Kruskal–Wallis test followed by pairwise comparisons using Mann–Whitney U tests (with Holm’s sequential Bonferroni’s correction for multiple comparisons). Asterisks denote p values as follows: \* $p < 0.05$ , \*\*\* $p < 0.005$ , \*\*\*\* $p < 0.001$ ;  $n=5$  and  $9$  for ChR2- and ReaChR-MNs, respectively at week 1 (grey) and  $n=9$  and  $9$  for ChR2- and ReaChR-MNs, respectively 3 weeks post-differentiation (black). (G) Sample current-clamp traces from ESC-derived MNs at 1 week (grey) or 3 weeks (black) post differentiation. Membrane depolarisation was elicited with 500 ms pulses of increasing current injections to establish rheobase (H) Percentage of ESC-derived motor neurons exhibiting repetitive, adaptive or single firing patterns. (I) Mean action potential firing frequency over a 500 ms step plotted as a function of injected current amplitude above rheobase for ESC-MNs at 1 week (grey) or 3 weeks (black) post differentiation; lighter lines denote SEM. Comparison made between firing rates at 300 pA above rheobase; \*\*  $p < 0.01$  Mann-Whitney U test. (J) Representative voltage recordings of ChR2- and ReaChR-MNs at week 1 and 3 in response to 500 ms pulses of increasing illumination intensity. (K) Summary plot of repolarisation decay constant following cessation of illumination of ChR2- and ReaChR-MNs at week 3. Points and lines indicate mean and SEM, respectively.

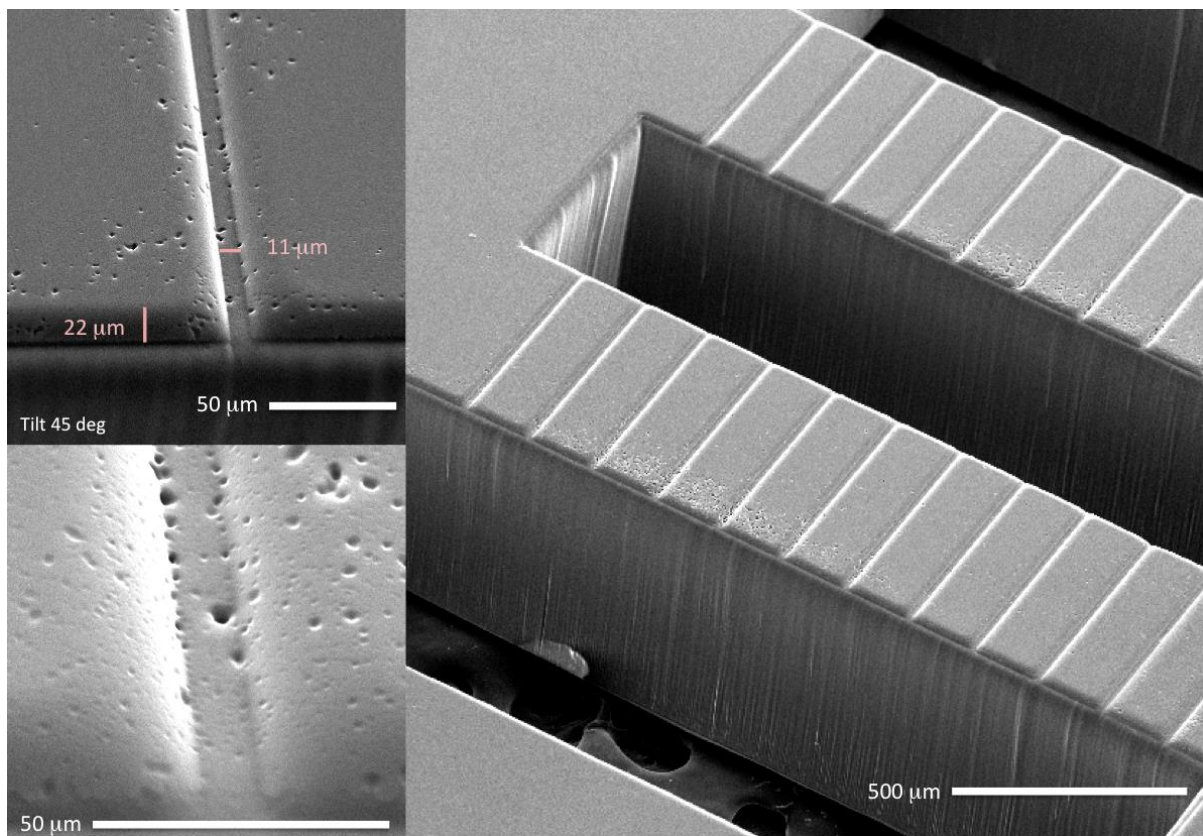


**Figure S4.** *Scanning electron microscopy analysis of the microdevice. The high-power images show microchannels. Scale bars – see individual images.*

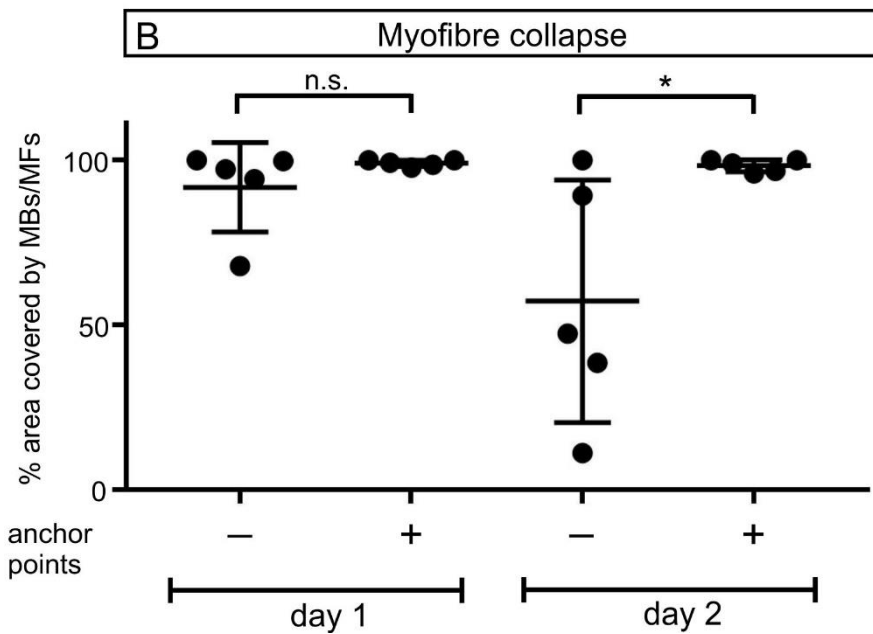
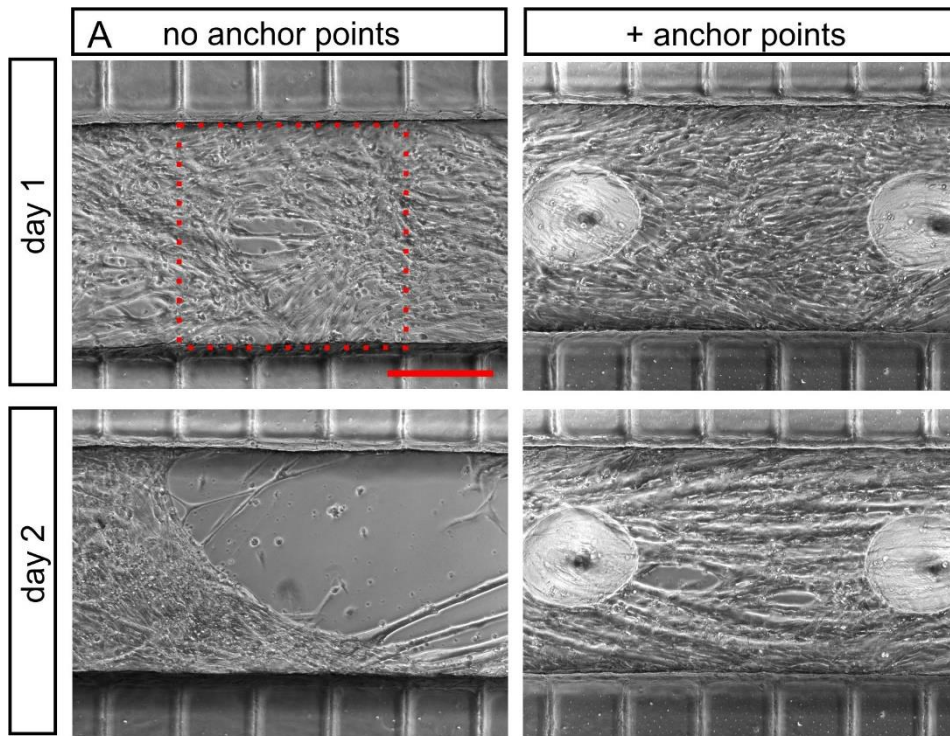


**Figure S5.** NOA-73 anchor points in the central compartment prevent myofibre collapse. (A) Chick myofibres were co-cultured with ChR2-MNs in devices with or without NOA-73 anchor points, and brightfield images of the central compartment were taken on day 1 and day 2. Myofibre collapse was quantified in the area between channels 5 and 8 (red rectangle). (B) The graph shows the quantification of the area covered by myoblasts/myofibres (n=5 separate devices per condition; unpaired t test, one-tailed p-value. \*p<0.05, n.s.: not significant). Scale bar 150µm. Lines indicate mean and SD.

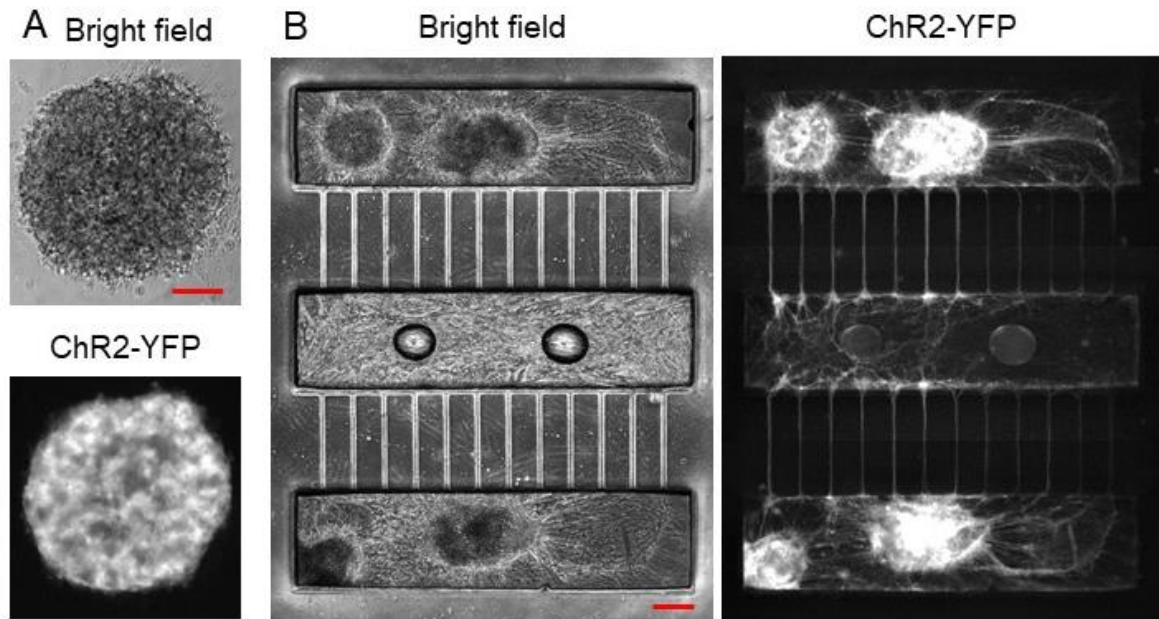


**Figure S6.** *Aggregation of ESC-MNs and ESC-ACs, and plating of aggregates into the compartmentalized microdevice. (A) 5000 ChR2-MNs and 5000 Gdnf-ACs were aggregated O/N into a 3D-sphere in low-adhesion U-bottom wells. ChR2-YFP labels MNs but not ACs. Scale bar 100  $\mu\text{m}$ . (B) Device loaded with three MN/AC aggregates each in the two outer compartments, and with myoblasts in the central compartment. The images were taken two days after plating the myoblasts. Both images are composites of three individual images each. Scale bar 200  $\mu\text{m}$ .*

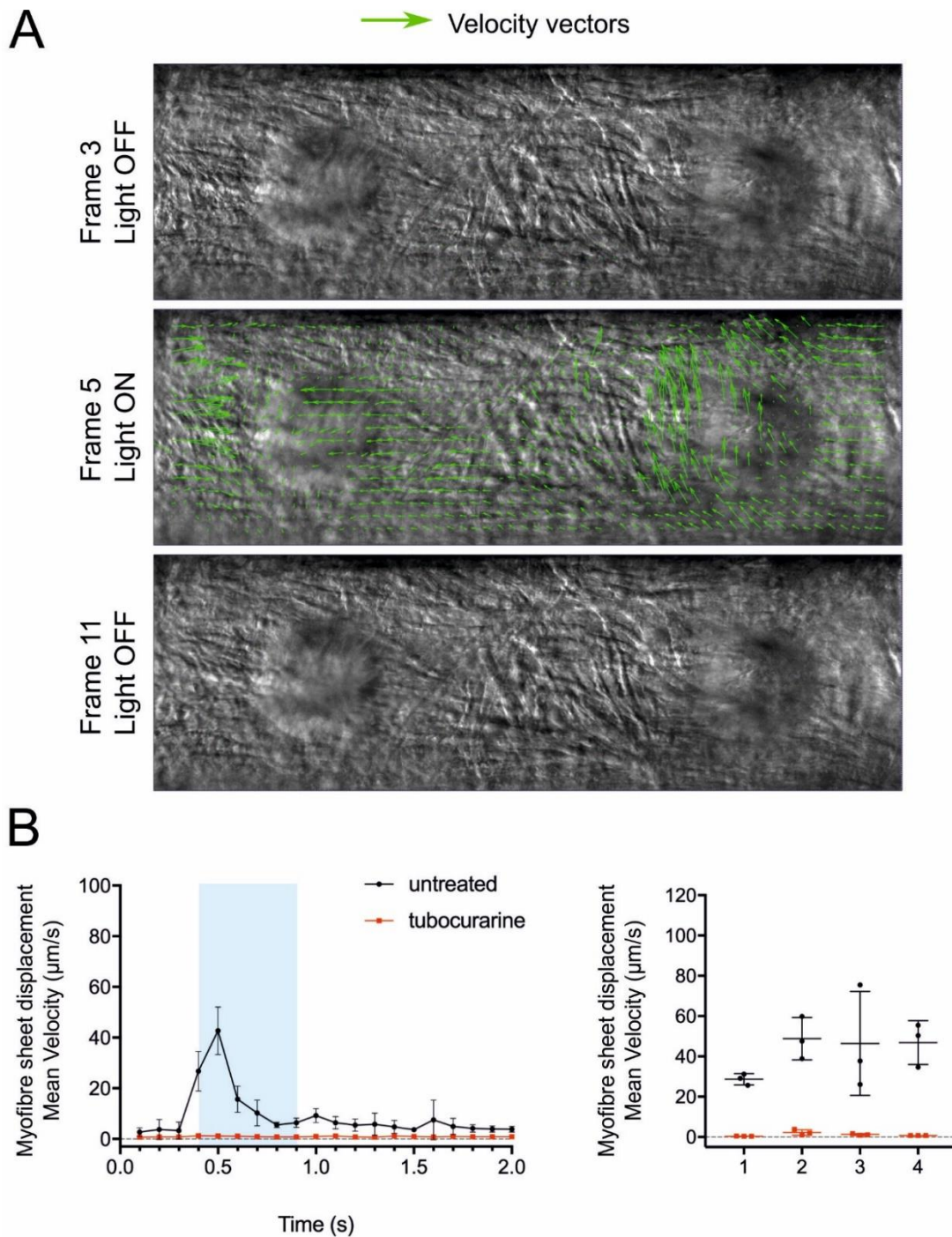


**Figure S7.** PIV analysis of muscle contraction induced by blue light stimulation of ChR2-MNs. (A) Frames were extracted from a recorded video before, during and after stimulation. Arrows represent the velocity vectors of myofibre displacement between 2 consecutive frames. (B) Myofibre contractions were recorded in devices containing ChR2-MNs in both sides of the central compartment. The blue box represents a 500 ms light stimulation. The graph on the right shows maximum mean displacement during light stimulation. Black and red lines represent cultures in medium without and with tubocurarine, respectively ( $n=4$  separate devices, each of them measured in triplicate). The time line of the experiment is the same as the one shown in Figure 4A. Error bars indicate SD.



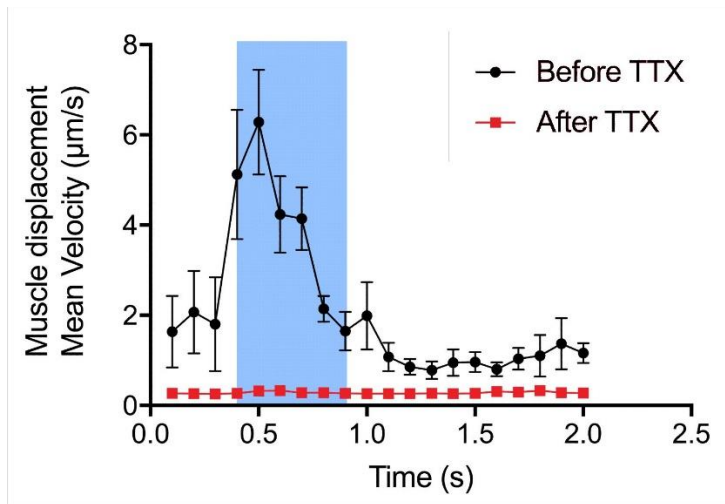


**Figure S8.** *TTX inhibits light-induced myofibre contractions.* Myofibre contractions were recorded in devices containing ChR2-MNs in both sides of the central compartment. The blue box represents a 500 ms light stimulation. The graph shows maximum mean displacement during light stimulation. Black and red lines represent cultures in medium without and with 1µM tetrodotoxin (TTX), respectively (n=4 separate devices, each of them measured in triplicate). The time line of the experiment is the same as the one shown in Figure 4A. Error bars indicate SD.

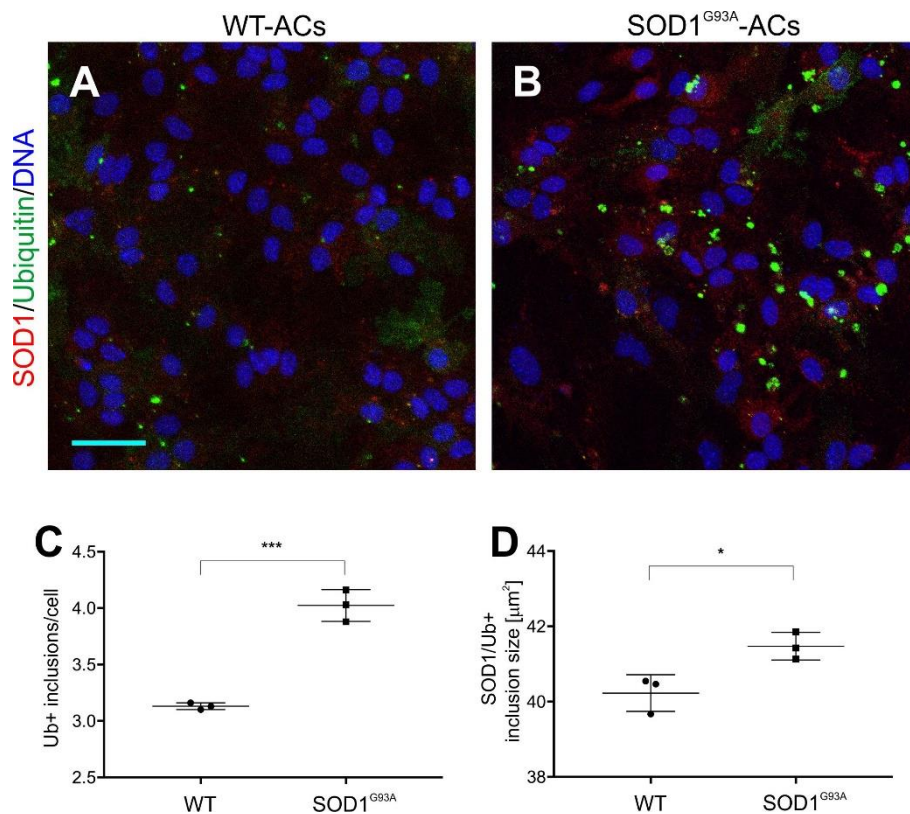


**Figure S9.** *SOD1<sup>G93A</sup> ACs show increased Ubiquitin-positive inclusions and increased size of SOD1/Ubiquitin+ inclusions.* (A) WT- and (B) SOD1<sup>G93A</sup>-ACs were differentiated, MACS-sorted and then culture for 1 weeks, fixed and then stained with antibodies for Ubiquitin and SOD1. Images of n=3 wells per condition were acquired with a Perkin Elmer Operetta system. (WT: 15305/15409/14630 cells; SOD1<sup>G93A</sup>: 12732/11415/9141 cells). Scale bar 50 μm. (C) The graph shows the number of Ubiquitin inclusions per cell in WT- and SOD1<sup>G93A</sup>-ACs. Unpaired t test, two-tailed p-value. \*\*\*p<0.001. (D) The graph shows the size of SOD1/Ubiquitin inclusions in WT- and SOD1<sup>G93A</sup>-AC cultures. Unpaired t test, two-tailed p-value. \*p<0.05. Lines indicate mean and SD.

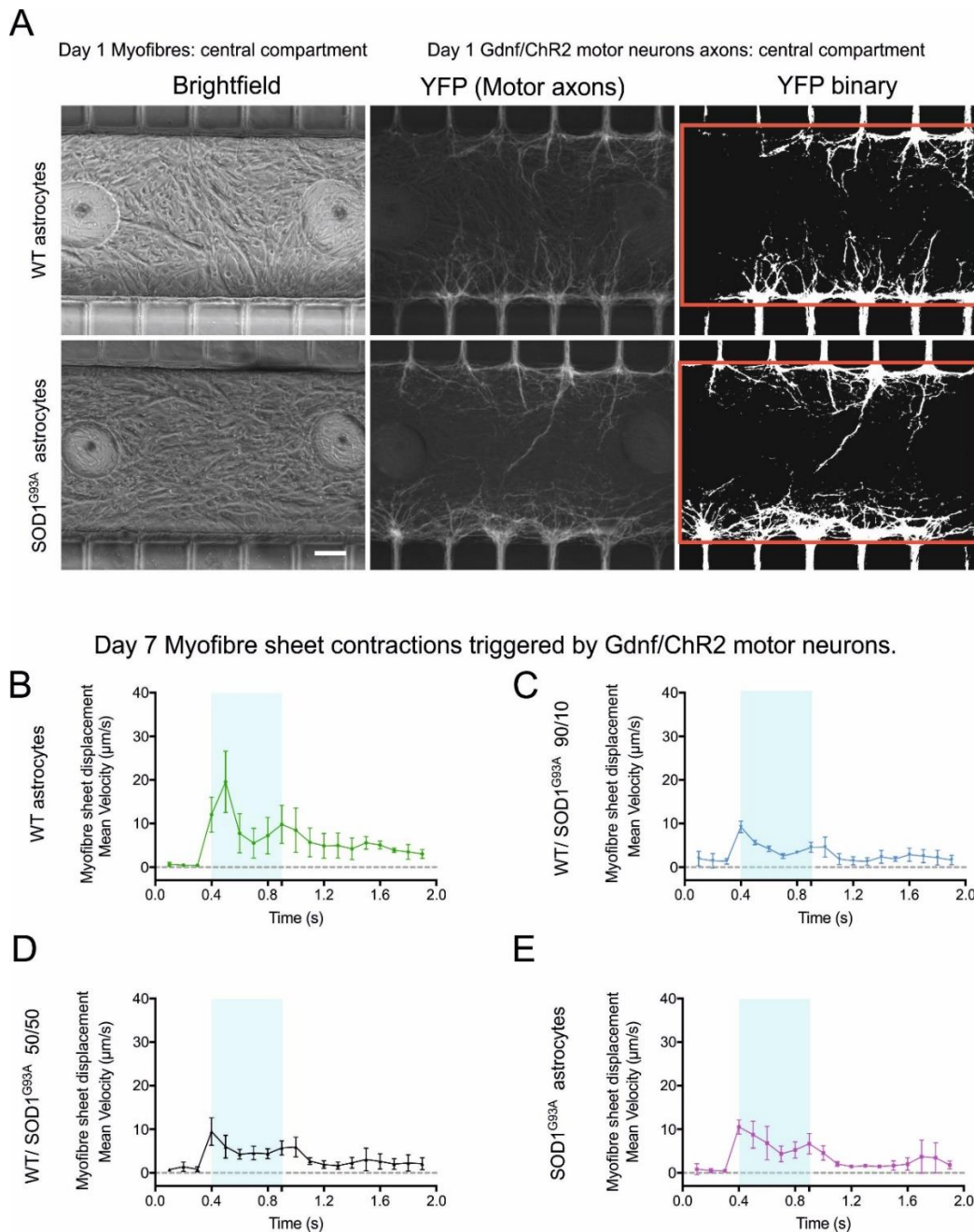


**Figure S10.** Motor axon outgrowth and myofibre contractions in co-cultures of Gdnf/ChR2-MNs with WT- and/or SOD1<sup>G93A</sup>-ACs. (A) Brightfield and YFP fluorescent images of central compartments on day 1. To determine motor axon outgrowth, the YFP fluorescent signal was transformed into a binary signal with ImageJ, and YFP+ pixels per area in the central compartment between microchannels four and nine (red frame) were quantified (n=5 devices for each condition). Scale bar 50 $\mu\text{m}$  (B-E) Myofibre contractions were recorded in devices containing Gdnf/ChR2-MNs co-cultured with WT- and/or SOD1<sup>G93A</sup>-ACs (see labels). The blue box represents a 500 ms light stimulation. Maximum mean displacement during light stimulation (n=3 (B, C) or n=4 (D, E) separate devices were measured in triplicate). Error bars indicate SD.

Primer		Sequence 5'-3'			
Mouse Gdnf forward		GCCGGACGGGACTCTAAGAT			
Mouse Gdnf reverse		CGTCATCAAACCTGGTCAGGATAA			
Mouse Sod1 forward		ATGGCGATGAAAGCGGTGT			
Mouse Sod1 reverse		CCTTGTGTATTGTCCCCATACTG			
Human SOD1 forward		GGTGGGCCAAAGGATGAAGAG			
Human SOD1 reverse		CCACAAGCCAAACGACTTCC			
Mouse Gapdh forward		AGGTCGGTGTGAACGGATTTG			
Mouse Gapdh reverse		TGTAGACCATGTAGTTGAGGTCA			
	Cq <i>Gapdh</i>	Cq mouse <i>Sod1</i>	dCq	dCq expression	ddCq expression relative to mouse <i>Sod1</i>
WT-ACs	16.18	17.50	1.32	0.40	1.00
SOD1 <sup>G93A</sup> - ACs	16.36	17.60	1.24	0.42	1.06
	Cq <i>Gapdh</i>	Cq human <i>SOD1</i>	dCq	dCq expression	ddCq expression relative to mouse <i>Sod1</i>
WT-ACs	16.18	undetected	n.a.	<u>n.a.</u>	<u>n.a.</u>
SOD1 <sup>G93A</sup> - ACs	16.36	17.10	0.74	0.60	<u>1.41</u>
	Cq <i>Gapdh</i>	Cq mouse <i>Gdnf</i>	dCq	dCq expression	ddCq expression relative to <i>Gdnf</i>
WT-ACs	20.20	31.73	11.53	0.00224278	1.00
SOD1 <sup>G93A</sup> - ACs	19.69	31.69	12.00	0.0013619	0.61
Gdnf-ACs	19.45	17.86	-1.59	15.7457378	7020.63

**Table S1.** *qPCR primer sequences and expression analysis.* Expression levels of mouse *Gdnf*, mouse *Sod1* and human *SOD1* in ESC-derived ACs were determined by qPCR. The gene expression level of *Gdnf* in WT-ACs was used as the baseline for *Gdnf* expression in Gdnf-ACs, and expression level of mouse *Sod1* in WT-ACs was used as the baseline for mouse *Sod1* and human *SOD1* expression in SOD1<sup>G93A</sup>-ACs; n.a. not applicable. Gene expression was normalised using expression of the housekeeping gene *Gapdh*. All qPCR measurements were performed in n=3 technical replicates.

Specificity 1° antibody	Host	Cat # / supplier	Dilution
Acetylcholine nicotinic receptor, muscle	Rat IgG	mAb 35 / DSHB	1:200
β3-tubulin (Tuj1)	Mouse IgG2a	MAB1195 / R&D Systems	1:500
CD14 (26ic)	Mouse IgG2b	HB-246 / ATCC	1:100
CD14-APC (M5E2)	Mouse IgG2a	555399 / BD Biosciences	1:50
Gdnf	Goat IgG	AF-212-NA / R&D Systems	1:500
GFAP	Rabbit IgG	Z0334 / Dako	1:1000
GFP	Rabbit IgG	A10262 / Invitrogen	1:1000
Glast (ACSA-1)	Mouse IgG2a	130-095-822 / Miltenyi	1:500
Isl1/2	Mouse IgG2b	39.4D5 / DSHB	1:500
SOD1	Rabbit IgG	ab13498 / Abcam	1:1000
Synaptic vesicle glycoprotein 2A	Mouse IgG1	SV2 / DSHB	1:500
Titin	Mouse IgM	9D10 / DSHB	1:200
Ubiquitin (P4D1)	Mouse IgG1	sc-8017 / Santa Cruz	1:500
Vimentin	Chick IgG	AB5733 / Millipore	1:10000

Specificity 2° antibody	Host	Type	Cat # / supplier
Rat IgG	Donkey	Secondary conjugated Alexa Fluor 405	ab175670 Abcam
Mouse IgG2a	Goat	Secondary conjugated Alexa Fluor 488 & 647	A21131 / A21241 Invitrogen
Mouse IgG2b	Goat	Secondary conjugated Alexa Fluor 647	A21242 Invitrogen
Goat IgG	Donkey	Secondary conjugated Alexa Fluor 568	A11057 Invitrogen
Mouse IgG	Donkey	Secondary conjugated Alexa Fluor 568	A10037 Invitrogen
Chick IgG	Goat	Secondary conjugated Alexa Fluor 488	A11039 Invitrogen
Mouse IgM	Goat	Secondary conjugated Alexa Fluor 568	A21043 Invitrogen
Mouse IgG1	Goat	Secondary conjugated Alexa Fluor 546 & 647	A21123 / A21240 Invitrogen
Rabbit IgG	Donkey	Secondary conjugated Alexa Fluor 488 & 568	A21206 / A10042 Invitrogen

Other reagents	Antigen	Type	Cat # / supplier
Bungarotoxin (BTX)	Nicotinic acetylcholine receptor	peptide conjugated to Alexa Fluor 555	B35451 Invitrogen

**Table S2.** Primary and secondary antibodies used in this study. Primary antibodies (top table) were incubated overnight at 4°C. Secondary antibodies (bottom table) were incubated at room temperature for 2 hours. All secondary antibodies purchased from Invitrogen were used at 1:1000 dilution; the anti-rat IgG-Alexa Fluor-405 secondary antibody (Abcam) was used at 1:200 dilution. BTX-Alexa-555 was used at 1:500 dilution.

**Supplemental Table S3.** *Details on statistical analysis.*

**Supplemental Videos.** *Quantification of myofibre contractions by PIV.* **S1:** Brightfield time-lapse video of the myofibre chamber for a 2 seconds interval at 10 frames/second, shown in real time. **S2:** This video shows the same time-lapse images as video S1 but slowed down five times to 2 frames/second.

## Abbreviations

Acetylcholine receptor	AChR
Advanced DMEM/Neurobasal/KOSR medium	ADFNK
Advanced DMEM/Neurobasal/NeuroBrew21 medium	ADFNB21
Amyotrophic lateral sclerosis	ALS
Astrocyte	AC
$\beta$ 3-tubulin	Tubb3
Bovine serum albumin	BSA
Bungarotoxin	BTX
Channelrhodopsin-2H134R	ChR2
Central nervous system	CNS
Dimethyl sulfoxide	DMSO
Embryoid body	EB
Embryonic stem cell	ESC
Fetal bovine serum	FBS
Fluorescence activated cell sorting	FACS
Glia-derived neurotrophic factor	Gdnf
Glial fibrillary axial protein.	GFAP
Green fluorescent protein	GFP
Knock-out serum replacement	KOSR
Induced pluripotent stem cell	iPSC
Light emitting diode	LED
Magnetic-activated cell sorting	MACS
Motor neuron	MN
Mouse embryonic feeder cells	MEFs
Neuromuscular junction	NMJ
Norland optical adhesive 73	NOA-73
Particle image velocimetry	PIV
Pluripotent stem cell	PSC
Polydimethylsiloxane	PDMS
Red-activatable Channelrhodopsin	ReaChR
Standard deviation	SD
Standard error of the mean	SEM
Superoxide dismutase-1	SOD1
Synaptic vesicle glycoprotein-2A	Sv2
Tetrodotoxin	TTX
Wild-type	WT
Yellow fluorescent protein	YFP

## Supplemental Experimental Procedures

### Compartmentalised device fabrication

The co-culture devices were manufactured by soft lithography, i.e. casting polydimethylsiloxane (PDMS) on a silicon mould. The mould, consisting of an array of positive patterns bearing the shape of the device (Figure 2), was prepared by photolithography. First, a layer of positive photoresist AZ5214 (Merck) was spun coated on a silicon wafer and exposed to UV light (31 mW/cm<sup>2</sup>, 5 seconds) all around the device features. The photoresist was developed with diluted AZ400K developer (Merck; 1:4; 3 minutes) and the wafer was etched to 10 µm depth using an ICP tool (Sentech). Secondly, three layers of SU8 2100 (Microchem) negative resist were deposited on the wafer to achieve a 600-700 µm height. The wafer was exposed to UV light (25 mW/cm<sup>2</sup>, 15 seconds) only above the rectangular compartments, avoiding the channels. The photoresist was developed with SU8 developer. As a result, each device replica on the mould comprised three 600-700 µm-high rectangles and arrays of 10 µm-high channels.

The mould was silanised overnight under vacuum with TriChloro (1H,1H,2H,2H-perfluorooctyl)silane (Sigma-Aldrich, 448931). The devices were then fabricated by casting PDMS (Dow Corning, Sylgard-184) onto the mould. Because the compartments had to remain open, care had to be taken to not pour too much PDMS on the mould, otherwise the devices would end up being sealed on top and not usable. The weight of PDMS to be cast on the wafer had to be adjusted to the optimal weight, 2.0 grams/wafer in our hands. The silicon mould was placed on a scale in a large Petri dish lined with aluminium foil and PDMS was poured over it in a controlled manner until reaching 2.0 grams. The mould was tilted until PDMS covered its entire surface, placed in a vacuum chamber, degassed for 20 minutes and PDMS was cured for two hours at 80°C. The PDMS was cut all around the wafer with a razor blade, carefully peeled off the mould with tweezers and transferred to a clean Petri dish (without inverting it) for inspection. In some devices a thin PDMS layer remained on the top and it was removed manually with tweezers. The resulting device had three open compartments.

The devices were then attached to 35mm glass-bottom dishes (Ibidi, 81158). The PDMS sheet was cut into small rectangles containing six (2x3) or nine (3x3)



devices each. Both the glass bottom dishes (without their lids) and the PDMS devices (on a tray, inverted with the channels facing up) were placed in a plasma cleaner (Femto, Diener Electronics). After five minutes of vacuum, the plasma was turned on for 30 seconds and vacuum was released. Immediately after, the devices were bonded to the dishes by flipping them over so that the channels were facing down and putting them in contact with the glass substrate. To increase bonding efficiency the devices were lightly pressed on the glass and placed on a hot plate at 70°C with a small weight (2g) on top of them for 60 minutes. At least one day after plasma bonding, two small NOA-73 (Norland Products) drops of approximately 150-200 µm diameter were applied to the bottom of the central compartment in register with microchannels 4 and 9. Liquid NOA-73 was pipetted with a glass capillary (WPI, TW150F-4) pulled on a Narishige PP-830 microelectrode puller and attached to an aspirator tube assembly (Sigma-Aldrich, A5177), and then UV-cured in a BLX-254 UV cross-linker (Vilber-Lourmat) for 1 minute, 55 J/cm<sup>2</sup>. Prior to cell plating, each device was UV-sterilised for 10 minutes, GFR-Matrigel (BD Biosciences, 356230) diluted 1:100 in DMEM (Gibco, 41966029) (1mL of diluted Matrigel solution) was added on top of the PDMS surface, and any air bubbles were flushed out of the chambers with a fine-tip pipette. The device with the coating solution was degassed in a vacuum chamber for 2 hours at room temperature, and then incubated for at least 20 hours at 4°C.

#### Generation of transgenic ESC clones

MN-ESC reporter clones *tol2-Hb9::CD14-IRES-GFP#13* (H14IG)<sup>[1]</sup>, *tol2-Hb9::CD14-IRES-GFP#13/tol2-CAG::ChR2-YFP#1A* (H14IG/CCRY), and *tol2-Hb9::CD14-IRES-GFP#13/tol2-CAG::ChR2-YFP#1A/PiggyBac-CAG::Gdnf#9* (H14IG/CCRY/CG), AC-ESC reporter clone *tol2-GFAP::CD14#H6* (G14) and plasmid *PiggyBac-CAG::GDNF/loxP-hygro-loxP* (Addgene, plasmid #78209)<sup>[2]</sup> were previously generated by our group. The coding region of *ReaChR*<sup>[3]</sup> was synthesised (GeneArt AG) and human *SOD1<sup>G93A</sup>* was obtained from Addgene (plasmid #26401). *PiggyBac-CAG::SOD1<sup>G93A</sup>/loxP-hygro-loxP* was generated by inserting a CAG promoter, *SOD1<sup>G93A</sup>*, a *bGH-polyA* site and a *loxP-hygro-loxP* cassette between the Sal1 and Xho1 sites in the polylinker of pXL-BACII<sup>[4]</sup>. The MN-ESC reporter clone carrying *PiggyBac-CAG::ReaChR-YFP/FRT-hygro-FRT* and the AC-ESC reporter

clones carrying *PiggyBac-CAG::Gdnf/loxP-hygro-loxP* or *PiggyBac-CAG::SOD1<sup>G93A</sup>/loxP-hygro-loxP*, were generated by co-transfecting PiggyBac donor constructs with p3xP3-DsRed1-orf PiggyBac transposase expression vector (kindly provided by Malcolm J. Fraser) by electroporation (Gene Pulser Xcell, Biorad) into ESC clones H14IG (*ReaChR-YFP*) or G14 (*Gdnf* and *SOD1<sup>G93A</sup>*), respectively. Recombinant ESC clones were selected with hygromycin (150 µg/mL - Invitrogen) on hygromycin-resistant mouse embryonic fibroblasts (MEFs) (Millipore, PMEF-HL) previously treated with mitomycin C (10µg/mL - Sigma, M4287), picked, expanded and screened for *Gdnf*, hSOD1<sup>G93A</sup> or *ReaChR-YFP* expression by immunocytochemistry and qPCR (Table S1). ESC clones *tol2-GFAP::CD14#H6/PiggyBac-CAG::Gdnf#6* (G14/CG), *tol2-GFAP::CD14#H6/PiggyBac-CAG::SOD1<sup>G93A</sup>#3* (G14/CS) and *tol2-Hb9::CD14-IRES-GFP#13/PiggyBac-CAG::ReaChR-YFP#B* (H14IG/RCY) were selected for subsequent experiments. All ESC clones used in this study are derived from IB10 (129/ola) ESCs<sup>[5]</sup>.

### Cell culture and differentiation

Mouse ESC culture was initially performed as described<sup>[1-2]</sup> (data in: Figures 1D, 6B, S2A-D and S3A-K). Due to problems with batch variations in MEFs and key components of the medium, we modified the ESC culture conditions as follows: Culture plates were coated with human recombinant laminin 521 (0.5 µg/mL - BioLamina, LN521) in PBS with Ca<sup>2+</sup> (Gibco, 14040091) for 1 hour at 37°C. ESCs were maintained in 2i/LIF medium [DMEM/F12 (Gibco, 11320033) and Neurobasal medium (Gibco, 21103049) mixed at 1:1 ratio and supplemented with N2 supplement (0.5x - Gibco 17502001), NeuroBrew21 without vitamin A (0.5x - Miltenyi, 130-097-263), 1:500 dilution of LIF supernatant (generated with COS7 cells transiently transfected with pCAG-LIF), L-glutamine (2 mM - Gibco, 25030081), plasmocin (5 µg/mL - InVivoGen, ant-mpt), penicillin/streptomycin (1x - Gibco, 15140122), 2-mercaptoethanol (55 µM - Gibco, 21985023), CHIR099012 (3µM - BioTechne, 4423/10), PD0325901 (1 µM - BioTechne, 4192/10), BSA fraction V (0.1% - Roche, 10735086001) and ES-qualified FBS (2% - Gibco, 16141061)]. ESCs were adapted to these feeder-free culture conditions for at least three passages. All ESC clones used in this study were tested for mycoplasma contamination with the

PCR Mycoplasma Test Kit I/C (Promocell, PK-CA91-1024) following the manufacturer's instructions and found to be mycoplasma-negative. Prior to mycoplasma testing, all ESC clones were cultured under feeder-free conditions for two passages in 2i/LIF medium without plasmocin, and supernatants were harvested when the cells reached 80-100% confluency.

For the experiments shown in Figures 1D, 6B, S2A-D and S3A-K, EBs were cultured for 5 days (MNs)<sup>[1]</sup> or 12 days (ACs)<sup>[2]</sup> in ADFNK medium<sup>[6]</sup> [Advanced-DMEM/F12 (Gibco, 12634010) and Neurobasal medium mixed at 1:1 ratio supplemented with L-glutamine (2 mM), 2-mercaptoethanol (55  $\mu$ M), knockout serum replacement (KOSR) (10% - Gibco, 10828028) and penicillin/streptomycin (1x)] supplemented with all-trans-retinoic acid (1  $\mu$ M - Sigma, R2625-50MG) and smoothed agonist (SAG) (0.5  $\mu$ M - Merck, 566660-1MG) from days 2 to 5. In all other experiments, the differentiation medium composition was modified: KOSR was substituted by a mixture of NeuroBrew21 (1x - Miltenyi, 130-093-566), N2 supplement (1x) and BSA fraction V (0.1%). This change was necessary, because we noticed a considerable degree of variability in MN yields when using KOSR. Culture in medium with NeuroBrew21-supplement (ADFNB21) led to more reproducible and increased MN yields (Figure S1). In contrast, medium with B27-supplement (1x - Gibco, 17504044), N2 supplement (1x) and BSA fraction V (0.1%) instead of KOSR was not superior to ADFNK medium. ESC-MNs and ESC-ACs were isolated by MACS using anti-CD14 antibody as described previously<sup>[1-2]</sup>, and analysed by flow cytometry with a FACS-Canto (BD Biosciences) at the Biomedical Research Centre, King's College London.

The measurement of MN survival on AC monolayers was carried out as follows: On day 0, 15k ESC-ACs and 200 ESC-MNs per well were plated in a 96-well format in ADFNK medium on Matrigel-coated wells. In some experiments, recombinant mouse Gdnf (10 ng/mL - Peprotech, 450-44) was added to the medium. To suppress the growth of contaminating proliferating cells, the medium was supplemented with 5-fluoro-2'-deoxyuridine/uridine (1  $\mu$ M each - Sigma, F0503/U3750) from day 1 onwards. Cultures were fixed with 4% PFA/15% sucrose on days 1, 3, 7, 14, 21, 28 and 35, washed with PBS, stained with anti-GFP antibody (Table S2), and the number of surviving MNs in each well was counted. MN survival

for each combination of MN and AC genotypes was assessed in three independent experiments in triplicate.

In order to measure ALS-like cellular pathology in WT- and SOD1<sup>G93A</sup>-ACs, the cells were MACS-sorted and then grown in triplicate wells as 2D-cultures on Matrigel-coated 96-well glass bottom plates (Perkin Elmer, 6005430) for 1 week, fixed and stained with Ubiquitin and SOD1 antibodies (Table S2). Plates were then imaged on a Perkin Elmer Operetta high content screening system. A pipeline was developed using the Harmony High Content Analysis software to count the number of cells, the number of ubiquitin inclusions and the size of SOD1/Ubiquitin colocalised inclusions.

Embryonic chick myoblasts were obtained by dissecting and isolating pectoralis muscles of E12 (ca. HH stage 38) White Leghorn chicks and incubating the muscle tissue for 30-60 min in dissociation buffer [collagenase I (0.2% - Gibco, 17100017) and DNase I (10 U/mL - Roche, 04536282001) in DMEM] in a water bath at 37°C. The tissue was then dissociated by repeated pipetting. The primary myoblasts were washed in PBS and cryopreserved in aliquots of ca. 10<sup>6</sup> cells in 90% FBS/10% DMSO.

### Electrophysiology

Whole-cell patch-clamp recordings were obtained from MACS-enriched ESC-MNs, cultured on Gdnf-expressing ESC-ACs for 7 and 21 days. MNs were visually identified using a BX51 Olympus microscope equipped with a 40X/0.8 N.A. water immersion objective (Olympus). The extracellular solution containing the following: NaCl (136 mM), KCl (2.5 mM), HEPES (10 mM), D-glucose (10 mM), CaCl<sub>2</sub> (2 mM) and MgCl<sub>2</sub> (1.3 mM), pH 7.4 with NaOH (280 mOsmol/L). Borosilicate thick-walled glass pipettes (3-5 MΩ) were filled with an internal solution containing the following: K-gluconate (130 mM), NaCl (10 mM), EGTA (1 mM), CaCl<sub>2</sub> (0.133 mM), MgCl<sub>2</sub> (2 mM), HEPES (10 mM), MgATP (3.5 mM), NaGTP (1 mM). Recordings were obtained at room temperature (22–25°C) with a Multiclamp 700B patch-clamp amplifier (Molecular Devices). Recordings were filtered at 3 kHz (eight-pole low-pass digital Bessel) and digitised at 10 kHz using a Digidata 1440A interface and pClamp10 software (Molecular Devices). Fast and slow capacitance transients were compensated for in the on-cell configuration. After switching to the current-clamp mode, action potentials were evoked either by 1 ms current injection so that the

injected current would not contaminate the action potential, or by 500 ms steps of increasing amplitude (5 pA increments) to establish rheobase. Light-triggered action potentials were evoked from MNs expressing either ChR2, or ReaChR following 500 ms of 470 nm light at 0.1-0.6 W/cm<sup>2</sup>, or 0.1-0.6 W/cm<sup>2</sup> of 635 nm light, respectively, using TTL-controllable LEDs (Prizmatrix). Electrophysiological data were analysed using the Neuromatic plugin for Igor Pro 6.10 (Wavemetrics), and custom written scripts in R. For information on the statistical analysis see Table S3.

### *In vitro* co-culture of MNs, ACs and myoblasts

MACS-sorted MNs and ACs were aggregated for 24 hours in U-bottom 96 well plates (Costar, 3799) previously coated with 0,5% wt/vol Lipidure-ethanol solution (50 µl/well - Amsbio, Lipidure-CM5206) under sterile conditions at room temperature overnight. Each well contained 10k cells in ADFNB21 medium (100 µl) and generated one aggregate. For experiments addressing the contribution of neural activity for synapse formation, we used aggregates formed with 5k MNs (H14IG or H14IG/CCRY) and 5k G14/CG-ACs. For experiments aimed at determining the effect of ACs expressing SOD1<sup>G93A</sup> on MNs, 5k H14IG/CCRY/CG-MNs were combined with WT-ACs (G14) and SOD1<sup>G93A</sup>-ACs (G14/CS) mixed at different ratios (100:0, 90:10, 50:50, 0:100) while keeping the total number of ACs constant at 5k. After plating of the cells into Lipidure-coated U-bottom 96-well plates, they were centrifuged at 200g for 1 minute and then placed in a tissue culture incubator.

On the following day, aggregates with the same MN and AC genotype combination were harvested with a multichannel pipette into a 10cm plate, transferred to a 15 mL tube and allowed to sediment for 5 minutes. The excess of medium was removed, and the aggregates were resuspended in ice cold ADFNB21 medium (100 µl). A hydrogel mix composed of fibrinogen solution (160 µl - Sigma, F8630 - 24mg/mL stock solution in 0.9% NaCl), GFR-Matrigel (40 µl) and 0.5M CaCl<sub>2</sub> (1 µl) was prepared and stored on ice. The suspension of MN/AC aggregates was combined with the hydrogel mix at a vol/vol ratio of 1:1 and transferred to a 35mm dish placed on ice. Sets of three aggregates were collected with P200 round gel-loading tips (StarLab UK, I1022-0610) and deposited in the upper and lower outer compartments (three aggregates per compartment) under a Leica MZ10F stereomicroscope. Aggregates were allowed to settle down by gravity for 5 minutes,

then thrombin solution (ca. 1  $\mu$ l - Sigma, T7513 – 50 U/mL in PBS/0.1% BSA) was pipetted into each (empty) central compartment, and thrombin (ca. 1 $\mu$ l) was added on the top of each outer compartment. The thrombin solution was released slowly from the narrow edges of the outer compartments to avoid disturbing the aggregates. Samples were incubated for 5 minutes at room temperature, plates filled with ADFNB21 medium (3 mL) and returned to the incubator.

Myoblasts obtained from E12 chick embryos were thawed and grown for 2 days in GFR-Matrigel coated plates with DMEM supplemented with FBS (20% - Sigma, F7524-500ML), Horse serum (10% - Gibco, 26050070), chick embryo extract (1% - SeraLab, CE-650-J), L-glutamine (2 mM) and penicillin/streptomycin (1x). One day after plating MN/AC aggregates into the devices (Figure 4A), myoblasts were dissociated with trypsin-EDTA (0.25% - Gibco, 25200056) for 5 minutes at 37°C and washed once in the growth medium and once in ADFNB21 medium. Cells were counted, and myoblasts were resuspended in ice cold ADFNB21 medium at 4-10k cells/ $\mu$ l. Myoblasts suspensions were combined 1:1 with freshly prepared hydrogel mix and kept on ice. Devices with MN/AC aggregates were taken from the incubator and the medium was removed until the top of the platforms was exposed. The medium in the central compartment and on top of the platforms was aspirated with P200 round gel-loading tips. Approximately 0.5 $\mu$ l of myoblast/hydrogel mix suspension (ca. 1-2.5k cells) was added into each central compartment under a stereomicroscope. To avoid trapping air bubbles, the cell suspension was slowly released into one end of the empty compartment. Cells were allowed to settle down for 5 minutes at room temperature and thrombin solution (ca. 1  $\mu$ l) was added on top of the central compartment from the narrow edges. After 5 minutes incubation at room temperature, plates were filled with ADFNB21 medium (3mL) and returned to the incubator. Starting 5 days after the plating of myoblasts (Figure 4A), MNs were stimulated (40% LED intensity, 20ms pulse at 5Hz) for 1 hour per day in dishes placed on top of a custom-built heat sink and LED assembly described in Wefelmeyer et al.<sup>[7]</sup>. During the light stimulation, the entire device was illuminated. ADFNB21 medium supplemented with an antioxidant cocktail (1x - Sigma, A1345) was added to the cells after each stimulation. After 5 days of stimulation, light-evoked muscle contraction was assessed by time-lapse imaging and synapse formation was evaluated by immunocytochemistry. For experiments aimed at

determining the effect of SOD1<sup>G93A</sup> ACs on MNs, the co-cultures were stimulated on day 5 and 6, and the analysis was performed on day 7 (Figure 6A). During the experiments aimed at determining the effect of light entrainment of ChR2-MNs on NMJ formation (Figure 5), the devices were shielded from light in 15cm petri dishes lined with aluminium foil. In some experiments aimed at reverting the MN phenotype induced by SOD1<sup>G93A</sup> ACs, the RIPK1 inhibitor Necrostatin-1 (10 $\mu$ M – Sigma-Aldrich, N9037) was added to the medium from day 1 onwards.

### Quantitative RT-PCR

ESC-ACs were MACS-sorted, and 50k cells per condition were cultured for 1 day. Their RNA was isolated using the PureLink RNA Mini kit (Ambion, 12183020), and cDNA was synthesised from extracted RNA with the GoScript Reverse Transcriptase System (Promega, A5003). Real-time qPCR reactions were prepared using the Power SYBR Green PCR Master Mix (Applied Biosystems, 4367659). PCR reactions were carried out in 384-well microamp plates with a Prism 7000 Sequence Detection System (Applied Biosystems). Cycling conditions were as follows: 50°C for 2 minutes (1x), 95°C for 10 minutes (1x), followed by 40 cycles of 95°C for 15 seconds, 60°C for 30 seconds and 72°C for 30 seconds, Primer sequences (Table S1) were obtained from the PrimerBank database<sup>[8]</sup>. Fold change in gene expression was measured as Cq (quantification cycle). qPCR analysis was carried out at the Genomics Centre, King's College London or at the Centre for Stem Cell & Regenerative Medicine, King's College London.

### Immunocytochemistry

EB sections and cell monolayers were fixed and processed as described previously<sup>[1]</sup>. To detect Gdnf protein in cultured ESC-ACs, the cells were cultured with brefeldin A (10 $\mu$ g/mL - Sigma, B7651) in medium for 1 hour prior to fixation. Co-cultures in microdevices were fixed with paraformaldehyde (PFA) in PBS (4% – Agar Scientific, R1026) at room temperature for 1 hour and washed with PBS twice. Samples were blocked, permeabilised and incubated with antibodies in PBD solution (3% BSA dissolved in PBS containing 0,1% Triton-X and 10% DMSO). Primary antibodies were incubated overnight at 4°C and secondary antibodies were

incubated for 2 hours at room temperature. All antibodies used in this study are listed in Table S2. Samples were washed in PBS-0.1% Triton-X three times of 15 minutes after each antibody incubation. Vectashield mounting medium (VectorLabs, H-1000) was added to the co-cultures prior to imaging.

Images were acquired using a confocal microscope (Zeiss LSM710 and LSM800, Nikon A1R) or an inverted fluorescence microscope (Olympus X73). Optical section stacks were processed with ImageJ software (<http://rsb.info.nih.gov/ij/>) and Bitplane Imaris 9.1.2.

Scanning electron microscopy of microdevices was performed at the Electron Microscopy Unit of the Mechanobiology Institute (NUS).

### Colocalisation analysis of pre- and postsynaptic structures

Synapses were labelled and measured in the central compartment with antibodies against synaptic vesicle-2 (Sv2, pre-synaptic/MN) and acetylcholine receptor (AChR, post-synaptic/myofibres). Additionally, an antibody against  $\beta$ 3-tubulin was used to label all axons and Chr2-YFP positive axons were identified based on the YFP fluorescence. Confocal z-stacks were taken from the microchannel exit area in both sides of the central compartment. Bitplane Imaris 9.1.2 was employed to quantify total area of  $\beta$ 3-tubulin, the size and number of pre- and post-synaptic structures as well as their colocalisation. Representative images of the area in the central compartment between 2-3 channels per cell type or condition were acquired for each device. The number of devices from which the measurements were acquired are shown in the Table S3. Using the Surface function in Imaris, 3D image volume of  $\beta$ 3-tubulin, Sv2, and AChR were created from z-stack images by a sequence of pre-processing, segmentation, and connected component labelling steps. Sv2 and AChR surfaces were used to get measurements of area, number and size of each labelled structure. The co-localisation analysis was performed using an automatic threshold run on both Sv2 and AChR channels using the ImarisColoc function. ImarisColoc employs Pearson's correlation coefficient (PCC) and Manders' Co-localisation Coefficients (MCC) to determine which voxels are colocalised and create a colocalisation channel. A new Surface based on the colocalised voxels was created allowing for the extraction of synapse features



(number and size). All measurements were exported to GraphPad prism for statistical analysis.

### Time-lapse Imaging

Brightfield time-lapse images were acquired using an inverted Olympus IX71 epifluorescence microscope with a 10x 0.25 NA oil immersion objective (Olympus). The devices were placed on a heated stage (Warner instruments) and maintained at near physiological temperature (32-35°C) throughout the recording. Time-lapse images were acquired at 10 Hz with a 100 milliseconds exposure using an ORCA-Flash4.0 V2 C11440-22CU scientific CMOS camera (Hamamatsu) cooled to 20°C with an Exos2 water cooling system (Koolance). Images were captured with HImage software (Hamamatsu), at 2048 x 2048 resolution. ChR2-expressing MNs were illuminated with a 500 milliseconds pulse of 470 nm light at 1.32 mW/cm<sup>2</sup> (measured at the specimen plane; CoolLED). The timing of the LED, and camera acquisition, were triggered externally through Clampex software (pClamp 10, Molecular Devices). Myofibre contraction velocity was quantified by Particle Image Velocimetry using the PIVlab package<sup>[9]</sup> within Matlab (MathWorks). Time-lapse movies acquired at a rate of 100 milliseconds per frame were analysed using three iterations of interrogation windows of 64/32/16 pixels, each with 50% overlap. Vectors were validated by filtering out velocity values higher than 7 times the standard deviation, the missing points were then replaced by linear interpolation values. Velocity magnitude representing the area mean value was exported for post analysis. In some experiments, synaptic transmission at the NMJ was blocked either with tubocurarine (50µM – Sigma-Aldrich, T2379) or tetrodotoxin (1µM – Acros Organics, 328560010).

## Supplemental References

- [1] C. B. Machado, K. C. Kanning, P. Kreis, D. Stevenson, M. Crossley, M. Nowak, M. Iacovino, M. Kyba, D. Chambers, E. Blanc, I. Lieberam, *Development* **2014**, *141*, 784-794.
- [2] J. B. Bryson, C. B. Machado, M. Crossley, D. Stevenson, V. Bros-Facer, J. Burrone, L. Greensmith, I. Lieberam, *Science* **2014**, *344*, 94-97.
- [3] J. Y. Lin, P. M. Knutsen, A. Muller, D. Kleinfeld, R. Y. Tsien, *Nat Neurosci* **2013**, *16*, 1499-1508.
- [4] X. Li, R. A. Harrell, A. M. Handler, T. Beam, K. Hennessy, M. J. Fraser, Jr., *Insect molecular biology* **2005**, *14*, 17-30.
- [5] E. Robanus-Maandag, M. Dekker, M. van der Valk, M. L. Carrozza, J. C. Jeanny, J. H. Dannenberg, A. Berns, H. te Riele, *Genes Dev* **1998**, *12*, 1599-1609.
- [6] H. Wichterle, M. Peljto, S. Nedelec, *Methods Mol Biol* **2009**, *482*, 171-183.
- [7] W. Wefelmeyer, D. Cattaert, J. Burrone, *Proceedings of the National Academy of Sciences of the United States of America* **2015**, *112*, 9757-9762.
- [8] A. Spandidos, X. Wang, H. Wang, B. Seed, *Nucleic acids research* **2010**, *38*, D792-799.
- [9] W. Thielicke, E. J. Stamhuis, *Journal of Open Research Software* **2014**, *2*.